Study of multi-carbide B_4C-SiC/(Al, Si) reaction infiltrated composites by SEM with EBSD

2014 IOP Conf. Ser.: Mater. Sci. Eng. 55 1200

(http://iopsc enc .iop or /1757-899X 55/1/012001)

IOP Conf. Series: Materials Science and Engineering **55** (2014) 012001 doi:10.1088/1757-899X/55/1/012001

Study of multi-carbide B_4C-SiC/(Al, Si) reaction infiltrated composites by SEM with EBSD

B A Almeida[1], M C Ferro[1], A Ravanan[1], P M F Grave[1], H-Y Wu[2], M-X Gao[2], Y Pan[2], F J Oliveira[1], A B Lopes[1] and J M Vieira[1]

[1] University of Aveiro, Department of Materials Engineering and Ceramics, Centre for Research in Ceramics and Composite Materials (CICECO), Campus Universitário de Santiago, PT-3810-193 Aveiro, Portugal
[2] Zhejiang University, Department of Materials Science and Engineering & State Key Laboratory of Silicon Materials, CN-310027 Hangzhou, P.R. China

E-mail: jvieira@ua.pt

Abstract. In the definition of conceptual developments and design of new materials with singular or unique properties, characterisation takes a key role in clarifying the relationships of composition, properties and processing that define the new material. B_4C has a rare combination of properties that makes it suitable for a wide range of applications in engineering: high refractoriness, thermal stability, high hardness and abrasion resistance coupled to low density. However, the low self-diffusion coefficient of B_4C limits full densification by sintering. A way to overturn this constraint is by using an alloy, for example Al-Si, forming composites with B_4C. Multi-carbide B_4C-SiC/(Al, Si) composites were produced by the reactive melt infiltration technique at 1200 - 1350 ºC with up to 1 hour of isothermal temperature holds. Pressed preforms made from C-containing B_4C were spontaneously infiltrated with Al-Si alloys of composition varying from 25 to 50 wt% Si. The present study involves the characterisation of the microstructure and crystalline phases in the alloys and in the composites by X-ray diffraction and SEM/EDS with EBSD. Electron backscatter diffraction is used in detail to look for segregation and spatial distribution of Si and Al containing phases during solidification of the metallic infiltrate inside the channels of the ceramic matrix when the composite cools down to the eutectic temperature (577 ºC). It complements elemental maps of the SEM/EDS. The production of a flat surface by polishing is intrinsically difficult and the problems inherent to the preparation of EBSD qualified finishing in polished samples of such type of composites are further discussed.

1. Introduction

Materials science can be represented by a tetrahedron of relationships with the fundamental vertices of composition, properties, processing and applications. In the definition of conceptual developments and design of new materials characterisation often takes a key role in clarifying what the new material is. Efforts to combine the great benefits obtained by the arrangement of metals and ceramics lead to development of composites. This takes a significant role in the modern industry where the permanent need to identify more economic and effective processing methods increases the research on composites.

Boron carbide (B_4C) is extremely hard, surpassed only by diamond and cubic boron nitride, and has unique properties such as low density (2.52 $g.cm^{-3}$), refractoriness, chemical inertness, thermal

stability and high hardness with abrasion resistance, making it the first choice for a wide range of applications [1]. Boron carbide has an atomic structure that can be described as composed of two atom arrangements: a primary structure formed by 12-atom icosahedra with B as the corners, linked by 3-atom C-B-C linear chains along the (111) rhombohedral axis, corresponding to the model stoichiometry of ($B_{13}C_2$), the icosahedra sitting on the vertices of a lattice with trigonal symmetry – space group $R\bar{3}m$; or in terms of an hexagonal lattice in which the [0001] direction axis matches the [111] rhombohedral direction [2]. B_4C structure has been extensively described in the literature [3-7] and although the crystal symmetry is obtained by diffraction methods, the resemblance in terms of nuclear scattering of boron and carbon atoms [8-9] makes almost indistinguishable the two atoms. Zoning of the B_4C solid solution displaying fluctuations of B/C ratio often yields $B_{13}C_2$-domains formed between B_4C zones of composition close to the $B_{12}C_3$ stoichiometry, the average size of the $B_{13}C_2$-domains being smaller than those of B_4C [10]. The zoned domains in the crystalline grains of the B_4C solid solution increase the difficulties of identification of diffraction pattern by automatic procedures as in electron backscatter diffraction (EBSD) results of B_4C which in the presence of Al as in the AA1100 - 16 vol% B_4C composite tend to be misidentified with the Al phase itself [11].

Disadvantages of the B_4C ceramics are the low self-diffusion coefficient, limiting densification by sintering and also brittleness, both being due to the covalent bonding of B_4C. Several methods were developed to prepare B_4C ceramics such as hot pressing [12-13] and pressureless sintering [14-15], however the extremely high temperatures needed of 2000 - 2200 ºC increase the global cost and make the materials less attractive. A way to overturn such inherent problems to produce useful materials based on B_4C is by using a different approach such as the infiltration method with a metal as infiltrate forming composites [1, 16-17].

Aluminium is an example of a metal that can be used to fill in the porosity of B_4C preforms. The low density of Al combined with high specific strength, easy machinability, good resistance to corrosion and high thermal and electrical conductivity, makes Al a coherent choice to use as infiltrate. In addition, Al-B_4C composites have low-cost casting for their production. However, the poor wettability of Al below 1000 ºC constitutes an obstacle for adequate mixing of the ceramic particles with the liquid phase [18-19]. It is possible to heat treat or coat the B_4C particles to improve the wettability factor [20] or control the formation of ternary phases of the Al-B-C system, of which nine ternary phases are known at least [21]. The alternative is alloying Al with other metallic elements such as Si making it more stable during infiltration. Si alloying also reduces the thermal expansion and improves mechanical properties of the alloy, mainly hardness [1].

The present study aims to characterize the microstructure and crystalline phases of the composites by X-ray diffraction and SEM/EDS with EBSD. It is part of the research work intending to evaluate the infiltration process, mostly on understanding the newly formed phases, specially the potential growth of ternary phases of Al-B-C rims on B_4C cores. It intends to look in detail for the segregation of Si in Al during solidification of the Al-Si metallic infiltrate constrained by the channels of the ceramic matrix when the composite cools down to the eutectic point (577 ºC, 12.5 wt% Si) [22].

2. Experimental procedure

As-supplied B_4C (Electron Microscopy Sciences EMS#50510-10, lot #BC80A22#36) powders with average particle size of 10 µm, and 99.9 % pure Al (ABCR GmbH & Co., CAS# 7429-90-5, lot# 143946-11) and 99.99 % pure Si (Emerk, Germany - 12497.0250, 201N628697), were used as raw materials. Fusion for production of smelted Al-Si alloys with Si content of 25 and 35 wt% was done at 1000 ºC - batches (1) and (2). Both processes, melting of the alloy as well as infiltration, were carried out on a graphite furnace under 50 kPa pressure of Ar gas above atmospheric pressure, with heating and cooling rates of 20 and 50 ºC/min, respectively. Batch (3) of the Al-Si alloy containing 25 wt% Si was smelted twice. Cylindrical pellets, 7.5 mm height, of the B_4C powders with polyvinyl alcohol (PVA) as binder were made by uniaxial pressing followed by isostatic pressing at 60 MPa and 196 MPa respectively, yielding green relative densities close to 50 %. Cut pieces of the Al-Si alloy in small chunks were pressed into cylindrical shapes and placed on top of B_4C preforms in amounts as

needed to fill the ceramic pore volume by reactive infiltration. Pressureless infiltration of the as-pressed preforms was carried on at 1200 °C, 1300 °C or 1350 ºC after a hold of 5 min to 1 h at the maximum infiltration temperature.

Density of the composites was evaluated by the Archimedes method in water. Crystalline phases were determined by X-ray diffraction (XRD, Rigaku) on polished surfaces of the Al-Si alloys and of the longitudinal cross-sections of the cylindrical pellets of the composites also used for SEM. Characterisation of the microstructure was performed by scanning electron microscopy (SEM, SU-70, Hitachi), combining elemental chemical analysis with energy-dispersive X-ray spectroscopy (high yield EDS, B-U Bruker QUANTAX 400) with analysis of crystalline phase distribution by electron backscatter diffraction (EBSD, Bruker CrystAlign QC 400). EBSD analysis is particularly sensitive to relief of surface finishing. For multiphase materials, in particular those containing phases of large differences of hardness, a final step of polishing with colloidal silica improves the finishing of the (soft) metallic phases, but it may also intensify the surface relief with negative effects on the hit rates of the EBSD analysis [11].

Mechanical polishing of the Al-Si alloy and of the composite was carried out by using diamond lapping papers of 30, 15, 9, 6 3 and 1 μm particle sizes. Surface finishing was done by a final step of polishing with colloidal silica suspension of 0.06 μm particle size for 60 minutes with light load of hand holding. In order to remove the plastically strained layer on the surface of the Al phase, the polished surfaces of the samples were submitted to a subsequent step of chemical etching at room temperature from 30 s to 1 min with a 25 % HNO_3 and 75 % methanol (vol%) solution, effective in the electrochemical polishing of aluminium [23]. By courtesy of Hitachi High-Technologies Europe GmbH (Krefeld, Germany), for comparison of finishing procedures one trial sample of the multi-carbide B_4C-SiC/(Al, Si) composite was mechanically polished and submitted to ion beam polishing for 70 minutes at 10º incident angle, 135 μA ion current in two steps: first 35 minutes with 4 kV accelerating voltage and a final step of 35 minutes at 6 kV. SEM observation, EDS and EBSD analysis of the samples of the Al-Si alloy and of ion beam polished surface of the composite were done without C coating. For the remaining surface finishing conditions of the composite samples light C coating was applied to eliminate electrical charging.

3. Results and discussion

3.1 Al-Si alloy

Figure 1 shows the X-ray diffraction results for the three alloys prepared as infiltrate for the composites. Batches (1) and (2) were prepared in same conditions, with just one melting step, and their difference is only in terms of composition, 25 and 35 wt% of Si, respectively. The third batch was prepared using a mixture containing 25 wt% Si, but in this case in two step melting, with double fusion. The main difference between the XRD spectrum of batches (1) and (3) is the absence of residues of Al_2O_3 oxide in the sample of the twice smelted Al-Si alloy.

Figure 2 gives the results of EDS/SEM and EBSD mapping for the Al-Si alloy of the twice smelted batch. The SEM image, figure 2a, and elemental mapping by EDS, figure 2b, indicate the formation of thin Si primary dendrites aside of the Al-rich phase. EBSD maps of the analysed area in figures 2c and d corroborate the EDS results. Figures 2c and d show many Si phase (~20 - 35 vol%) being detected in the Al areas, and this is due to the software that is unable to select clearly the right Al phase. There is also number of misindexing points in the Si phase. From the automated image analysis by the EBSD software there is 6 and 11 % zero solutions (black dots) in the results of figures 2c and d, respectively. This means that the system could not index any of the available phases on such points. The map in figure 2d, obtained after chemical etching, shows the increase of zero solutions. Although short, the time of chemical etching, 30 seconds, could have been too long. The elemental composition of the Al phase was determined by quantitative standardless EDS analysis after energy calibration of the detector, with the fixed gauge area as given in red in figure 2a in red. Up to five EDS spectra were collected on different areas of the Al matrix, yielding the average composition of

98 ± 1 at% Al (the remaining being Si). This value overlaps with the solid solution limit of α-Al (1.65 wt% Si) [22].

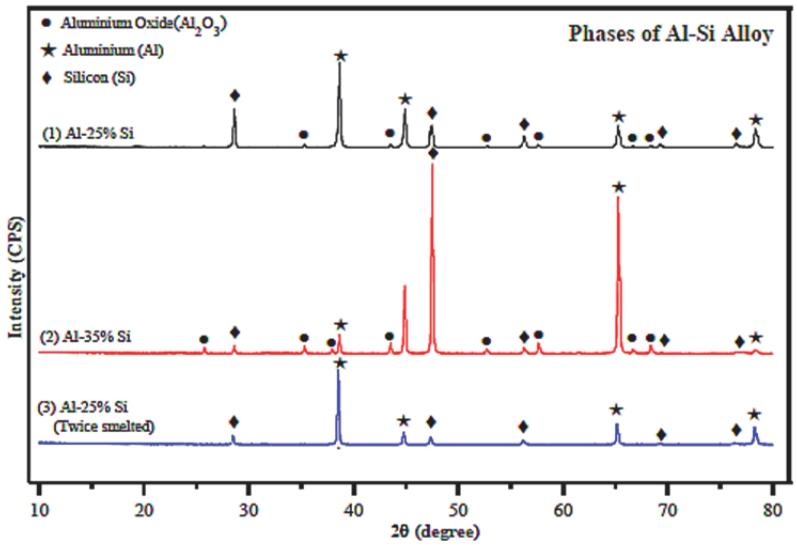

Figure 1. XRD results for the three Al-Si alloys prepared by varying the composition and/or the melting process.

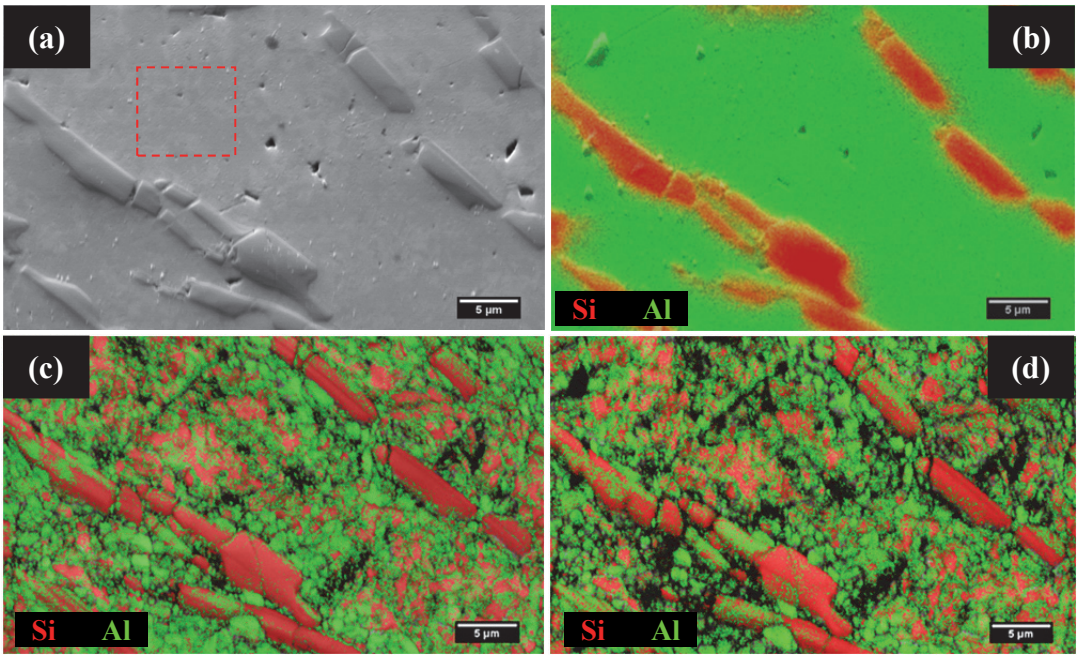

Figure 2. Analysis of microstructure and composition of the twice smelted Al-25 wt% Si alloy: (a) SEM microstructure with region selected for EDS quantification in red; (b) EDS elemental map; EBSD phase map for the alloy (same colour code as in b); (c) before chemical etching; and (d) after chemical etching (map area of 83.7 x 62.78 µm^2 with 0.065 µm step size).

From the EBSD report, the composition of the Al-Si alloy for the total area as shown in figure 2 ranges from 35 vol% of Si phase for the as polished surface in figure 2c to 40 vol% of Si phase after the chemical etching, figure 2d; these values being not far away from the elemental composition of 32 ± 2 at% Si from EDS analysis. As the solid solubility of Al in the Si crystalline lattice is very low [22], these results are significantly above the average Si content of the alloy of 22 vol% Si phase. The composition of the small area sampled in figure 2 neatly deviates from the average composition of the alloy. The results of XRD analysis should probably be more accurate than those of SEM with EDS or EBSD analysis as a much wider volume and more representative of the composition of the sample is analysed by XRD.

The discrepancies that persist between the Al phase content of the alloy obtained from the EBSD analysis compared to the EDS results can be attributed to disturbing effects of low temperature passivation of the Al surface forming a 2 - 4 nm thick amorphous oxide layer [24] that cannot be resolved by EBSD, to smearing of the surface layer from plastic deformation during polishing that blurs the Kikuchi line patterns [11] and to the relief of the surface. The thickness of the passivation layer of Al being a minor fraction of the backscattered electron interaction depth [25], the resulting perturbation of EBSD identification is seemingly minute. Protrusion of the hard Si particles of the alloy and of Si and B_4C particles of the composites can shadow the Al phase once the electron beam intersects the high angle tilted sample. Both the Al and Si phases have face-centred cubic crystalline lattices, the Al belonging to the $Fm\bar{3}m$ space group with a_0 = 4.05 Å and the Si to the $Fd\bar{3}m$ space group with a_0 = 5.43 Å. The likeness of lattice constants and space groups of Al and Si may also explain the difficulty of the EBSD technique to distinguish between these phases. Such resemblance can mislead the EBSD software to select Si instead of Al as the correct phase in significant proportion of the hits. Hence changes in the EBSD resolution associated to smearing or surface relief would necessarily conduct the EBSD software to confuse the identification of the phases in increasing rates. But, the failure of EBSD to correctly index the Al phase may also come from the presence of sub-grains in the Al phase originated from the rapid solidification [26]. Figure 3a displays the grain orientation in X direction with inverse pole figures for both Si and Al phases, the size histogram of the Al phase being given in figure 3b, a fine sub-grain structure being observed inside the Al-rich matrix.

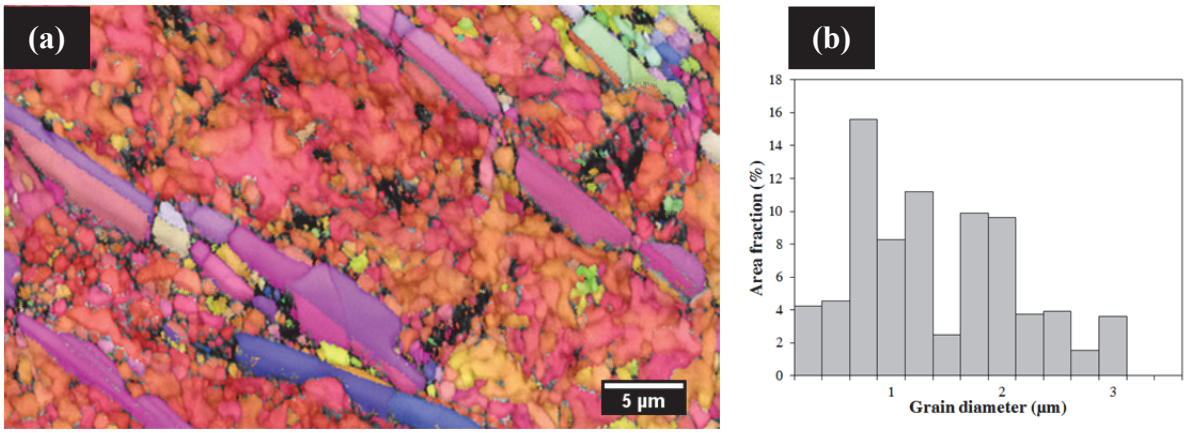

Figure 3. (a) Inverse pole figure in X direction (IPF-X) of figure 2; and (b) the size histogram of the Al phase on an area of approximately 83.7 x 62.78 µm^2, 0.065 µm step size.

The histogram in figure 3b shows that the metallic matrix of Al is largely constituted by fine domains with sizes ranging from 0.25 to 2.0 µm. The particles with sizes above this threshold seen in figure 3a are mainly Si primary dendrites. The fine sub-grain size of the α-Al solid solution is an additional difficulty for crystalline phase identification by EBSD in SEM. This becomes even more

relevant on composite structures constituted by many phases. The need for more studies to understand the effect of the sub-micrometre grain sizes on EBSD phase mapping is acknowledged in the bibliography [11, 26].

3.2 Multi-carbide B_4C-SiC/(Al, Si) composites

In order to evaluate the distribution of crystalline phases through the sample, the composite was cut in 3 parts along the axis of the cylindrical pellet for the XRD analysis: top of infiltration (entry of metal), middle and bottom (end). Figure 4 presents the XRD results for composite "C" in the three analysed regions. Analysis of XRD diffractograms using standards shows that the four main phases of the composite have volume fractions close to the following: Al (44 vol%), Si (19 vol%), B_4C (33 vol%) and SiC (4 vol%). The volume fractions were converted to the molar fractions given in the first row of Table 1 with the values of molecular weight and density of each phase.

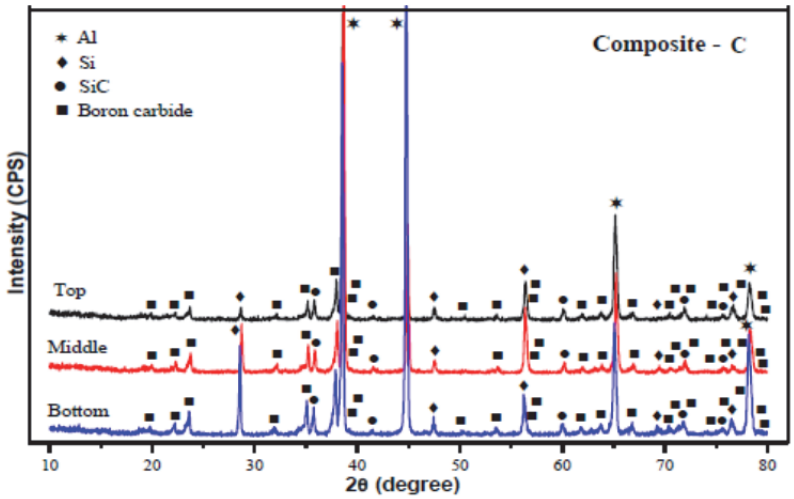

Figure 4. XRD results of composite "C" in three regions: top of infiltration, middle and bottom (end).

Table 1. Molar fraction of main crystalline phases of the B_4C-SiC/(Al, Si) composite determined from XRD analysis and calculated by EBSD image analysis.

	Al	Si	B_4C	SiC	Zero solutions
XRD analysis (mol %)	56.4	20.2	19.3	4.1	---
Figure 5 phase map (d) (vol%)	31.3	27.8	38.8	2.1	24.9 %
Figure 5 phase map (f) (vol%)	39.4	18.6	38.4	3.6	33.0 %

The microstructure of the same multi-carbide B_4C-SiC/(Al, Si) composite "C", with surface finishing obtained by two methods, conventional polishing with chemical etching and ion beam polishing, are presented in figure 5. Elemental maps for Al, Si and B of the composite are displayed in figures 5b and c. EBSD phase maps for conventional polished and ion beam polished surfaces are exhibited in figures 5d and e, respectively. The EBSD analysis of the composite was performed with the intent of determining the segregation of the Si phase from the Al during solidification of the metallic infiltrate inside the channels of the ceramic matrix when the composite cools to the eutectic point (577 ºC). The results of the corresponding reports on phase composition based on the EBSD

image analysis are given in Table 1. The volume fraction of the phases from EDSD results of the chemically etched sample and ion beam polished sample rank the phase content by the same order, but the Al is detected in relatively lower amounts than by the XRD whereas the opposite is observed for the B_4C phase.

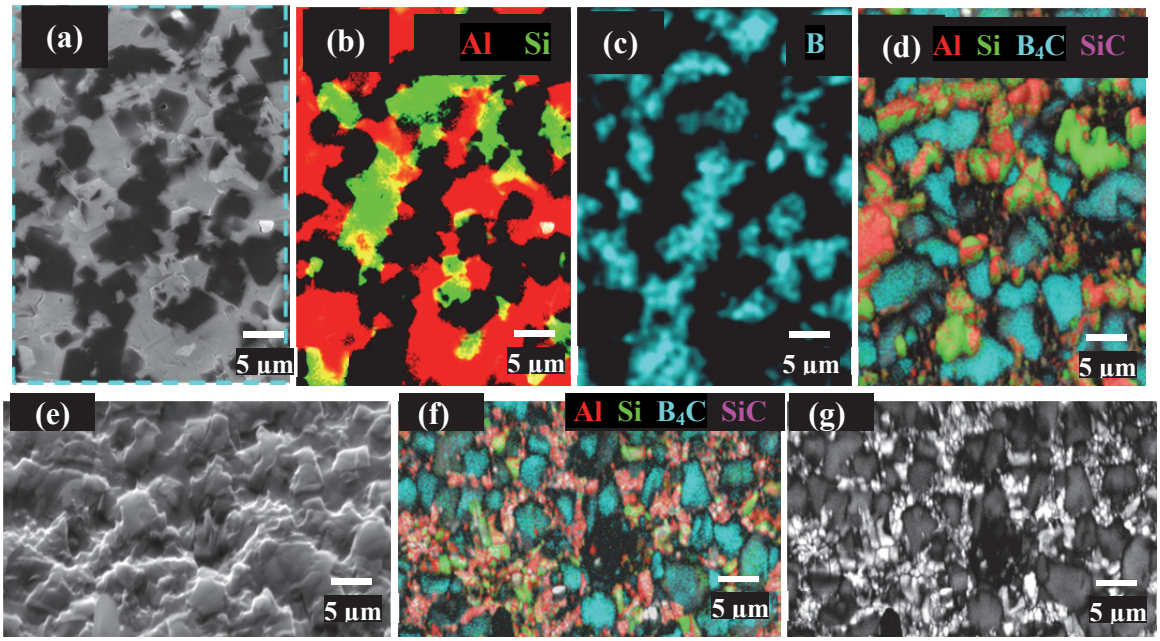

Figure 5. Multi-carbide B_4C-SiC/(Al, Si) composite. (a) - (d) polished section of with chemical etching: (a) SEM microstructure; (b) - (c) Elemental maps from EDS to Al+Si and B; (d) EBSD analysis for Al, Si and B_4C, with area of 46.5 x 33.9 μm^2 and 0.082 µm step size; (e) - (g) polished section with ion beam polishing: (e) SEM microstructure; (f) EBSD phase map for Al, Si and B_4C; and (g) the pattern quality map, with area of 47.5 x 40.6 μm^2 and 0.082 µm step size.

The constrains of the mechanical polishing technique with chemical polishing to improve surface quality to the level needed for EBSD analysis of a four-phase composite may seemingly be lessened by using ion beam polishing (or direct cross section) for the same purpose [11, 27].

The quality of EBSD data of the composite sample was also improved by adjusting the main controls of operation of the SEM: accelerating voltage (V_{acc}) and current emission (I_e). By increasing V_{acc}, the intensity of available signal is larger, but the size of the interaction volume between the electron beam and sample is also enlarged, decreasing spatial resolution of EBSD in conflict with the need to index the small (often sub-micrometre sized) grains of the Al and Si phases in the narrow spaces between B_4C particles. In SEM-EDS, due to high capability of X-rays to penetrate matter, the calculated depth of the interaction volume for 20 kV electron beam is 3.1 µm while for 15 kV it decreases to 1.9 µm, as calculated for applied EBSD conditions (incident beam at 70º, 27 mm work distance) and composition of the composite determined by EDS in the area of figure 5e. Differently, backscattered electrons are generated in the near surface layers of the sample, decreasing therefore the depth of backscattering to 10 - 20 nm, the large fraction of useful EBSD signal being emitted from this volume [28].

A larger overlap with blur of Kikuchi lines at high V_{acc} may prevent the correct indexing of phases with similar crystalline structures. Otherwise, I_e can be increased by changing the objective lens aperture to a larger one thus intensifying the available signal. The effect of varying the two SEM

operation controls, V_{acc} and I_e, on EBSD image quality for Al phase is illustrated in the images of figure 6.

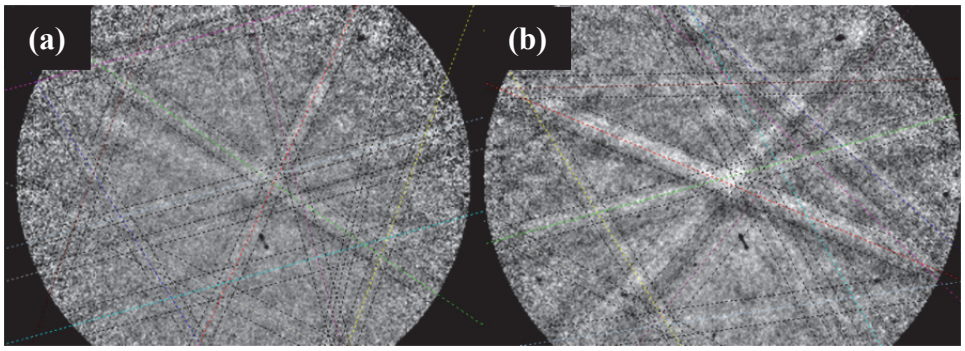

Figure 6. Kikuchi diffraction pattern for the same micrometre-sized crystal of the Al phase and approximately fixed position inside the grain with different SEM operation conditions: (a) V_{acc} = 20 kV and 0.086 nA probe current (50 µm objective lens aperture); (b) V_{acc} = 20 kV and 0.194 nA probe current (100 µm objective lens aperture).

Due to the unresolved issues, it was not possible to make the identification if Al-B-C rims or ternary phases formed on B_4C cores by using EBSD in SEM up to the present stage of this study. Two directions for future work emerge from the present study. The improved spatial resolution down to nanometre range of the SEM-TKD technique, transmission Kikuchi diffraction in the SEM microscope, as compared to SEM-EBSD [24, 29], will expectedly aid the automated recognition of electron diffraction patterns of the Al and Si phases with sub-grain structures of submicron sizes. But, for SEM-TKD the sample has to be prepared as a thin section of transmission electron microscopy.

The Al phase plays a key role in toughening of the B_4C-SiC/(Al, Si) composites [1]. Aligned with the broad objectives of the study, the assessment of fracture toughness of the composite by indentation fracture and demonstration by EBSD techniques of the extent of plastic deformation in crack-bridging Al particles contributing to the fracture energy demands at the same time samples with dimensions large enough for the indentation fracture tests but with surfaces rectified and polished to EBSD quality.

4. Conclusions

Multi-carbide B_4C-SiC/(Al, Si) composites were prepared by the reactive melt infiltration method from the B_4C porous preforms, with Al-Si alloy at temperatures between 1200 and 1350 ºC under Ar atmosphere. The study of microstructure and composition of the Si-Al alloy and the composites by XRD and SEM/EDS with EBSD analysis lead to the following conclusions:

a) Present results corroborate other studies on polishing of composite materials by conventional mechanical methods for EBSD analysis; the method applied to the Al-Si alloy and to composites of this study gave quality enough for EBSD characterisation after chemical polishing. Limited by the constraints of surface relief and resemblances of crystallography of main phases of the composite, namely of the Al and Si crystalline lattices, the automated software was unable to select clearly the right Al phase in many points, or conversely the Si phase, and the reliable quantification of phases by EBSD especially of the Al phase was not feasible in spite of much better EBSD spatial resolution than the EDS one.
b) Plastic smearing more than passivation of the Al surface layer, small (sub-micrometre) sub-grain structures combined with surface relief can explain the difficulty of indexing this phase in the

composites by the automated software of phase recognition of EBSD. Chemical etching of the polished surface for up to 1 minute improved in part the indexing of Al by EDSD.

c) Ion beam polishing also improved the finishing of the cross-sections of the composite for the use in EBSD analysis. But, the noticeable increasing of relief stand for further study particularly directed to find proper conditions for preparation of low relieve polished surfaces from multi-phase materials with a large span of hardness of their phases.

Acknowledgments
The authors would like to acknowledge the RNME - Pole University of Aveiro (FCT Project REDE/1509/RME/2005) for access to SEM microscopy, the scientific and technical assistance and one of the authors the EMMS consortium funded by the European Commission for the M.Sc.-scholarship.

References

[1] Wu H, Zhang S, Gao M, Zhu D, Pan Y, Liu Y, Pan H, Oliveira F J and Vieira J M 2012 *Mater. Sci. Engng. A* **551** 200-208
[2] Domnich V, Reynaud S, Haber R A and Chhowalla M 2011 *J. Am. Ceram. Soc.* **94** 3605-3628
[3] Lipp A 1996 *Tech. Rundsch.* **58** [7] 1-47
[4] Thavenot F 1990 *J. Eur. Ceram. Soc.* **6** 205-225
[5] Vast N, Sjakste J and Betranhandy E 2009 *J. Phys. Conf. Ser.* **176** 012002
[6] Suri A K, Subramanian C, Sonber J K and Murthy T 2010 *Int. Mater. Rev.* **55** 4-11
[7] Werheit H, Filipov V, Kuhlman U, Schwarz U, Armbruster M, Lei-the-Jasper A, Tanaka T, Higashi T, Lundstrom T, Gurin V N and Korsukova M M 2010 *Sci. Technol. Adv. Mat.* **11** 023001
[8] Morosin B, Kwei G H, Lawson A C, Aselage T L and Emin D 1995 *J. Alloy. Compound*. **226** 121-125
[9] Jiménez I, Sutherland D G J, van Buuren T, Carlisle J A, Terminello L J and Himpsel F J 1998 *Phys. Rev. B* **57** 13167-13174
[10] Schwetz K A and Karduck P 1991 *Boron-rich solids*. Vol. 231 (Emin D, Aselage T, Beckel C L, Switendick A C and Morosin B; Eds.) (New York: American Institute of Physics)
[11] Guo J, Amira S, Gougeon P, Chen X-G 2011 *Mater. Charact.* **62** 865-877
[12] Li A J, Zhen Y H, Yin Q, Ma L P, Yin Y S 2006 *Ceram. Int.* **32** 849-856
[13] Zorzi J E, Perottoni C A and Da Jornada J A H 2005 *Mater. Lett.* **59** 2932-2935
[14] Mashhadi M, Taheri-Nassaj E, Sglavo V M, Sarpoolaky H and Ehsani N 2009 *Ceram. Int.* **35** 831-837
[15] Miyazaki H, Zhou Y, Hyuga H, Yoshizawa Y and Kumazawa T 2010 *J. Eur. Ceram. Soc.* **30** 999-1005
[16] Hayun S, Rittel D, Frage N and Dariel M P 2008 *Mater. Sci. Eng. A* **487** 405-409
[17] Mizrahi I, Raviv A, Dilman H, Aizenshtein M, Dariel M P and Frage N 2007 *J. Mater. Sci.* **42** 6923-6928
[18] Lin Q L, Shen P, Qiu F, Zhang D and Jiang Q H 2009 *Scripta Mater.* **60** 960-963
[19] Toptan F, Kilicarslan A, Karaaslan A, Cigdem M and Kerti I 2010 *Mater. Design* **31** S87-S91
[20] Kennedy A R and Brampton B 2011 *Scripta Mater.* **44** 1077-1082
[21] Halverson D C, Pyzik A J, Aksay I A and Snowden W E 1989 *J. Am. Ceram. Soc.* **72** 775-780
[22] Warmuzek M 2004 *Aluminum-silicon casting alloys - Atlas of microfractographs*. (ASM International, 2
[23] Ünlü N 2008 *Mater. Charact.* **59** 547-553
[24] Eisenreich N, Fietzek H, Juez-Lorenzo M M, Kolarik V, Koleczko A and Weiser V 2004 *Propellants, Explosives, Pyrotechnics* **29** 137-145
[25] Keller R and Geiss R H 2012 *J. Microsc.* **245** 245-251

[26] Humphreys F J, Huang Y, Brough I and Harris C 1999 *J. Microsc.* **195** 212-216
[27] Schwartz A J, Kumar M, Adams B L and Field D P 2009 *Electron backscatter diffraction in materials science - 2nd Edition*. (Springer)
[28] Winkelmann A 2010 *J. Microsc.* **239** 32-45
[29] Trimby P W 2012 *Ultramicrosc.* **120** 16-24